

## Original Article

## Neuroprotective Effect of Allogeneic Biomaterial on Rat Neocortex After Its Intramuscular Injection



Anna Ivanova Lebedeva<sup>1</sup> , Evgeny Musinovich Gareev<sup>1</sup> , Lyalya Akhiyarovna Musina<sup>1</sup> , Alexey Viktorovich Prusakov<sup>2\*</sup> , Anatoliy Viktorovich Yashin<sup>2</sup> , Vladimir Sergeevich Ponamarev<sup>2</sup>

1. Federal State Budgetary Educational Institution of Higher Education, Bashkir State Medical University, Ministry of Health of the Russian Federation, (All-Russian Center for Eye and Plastic Surgery), Ufa, Russia.

2. Federal State Budgetary Educational Institution of Higher Education, Saint Petersburg State University of Veterinary Medicine, Saint Petersburg, Russia.



**How to Cite This Article** Lebedeva, A. I., Gareev, E. M., Musina, L. A., Prusakov, A. V., Yashin, A. V., & Ponamarev, V. S. (2025). Neuroprotective Effect of Allogeneic Biomaterial on Rat Neocortex After Its Intramuscular Injection. *Iranian Journal of Veterinary Medicine*, 19(1), 31-40. <http://dx.doi.org/10.32598/ijvm.19.1.1005479>

<http://dx.doi.org/10.32598/ijvm.19.1.1005479>

**ABSTRACT**

**Background:** Forced physical activity violates all organ and system interactions. Allogeneic biomaterial has been used for many years for regeneration, but its remote exposure has not been studied.

**Objectives:** The aim of this research is the morphological study of experimental animals' precentral gyrus neocortex under forced physical activity and after intramuscular injection of allogeneic biomaterial.

**Methods:** Male Wistar rats were used for the experiment. The Porsolt test or despair test was used for 30 days. In the main group (n=10), after 30 swimming sessions, allogeneic biomaterial (BMA) was injected intramuscularly. In the control group (n=10), the animals were injected with saline in the same volume. Then, 5 and 21 days after the injections, a tolerance load test was performed, after which the animals were taken out of the experiment by insufflation of a lethal dose of chloroform vapors. Their brains were removed, and morphological studies were performed.

**Results:** In the experimental group, 5 days after the BMA injection, the median level of the multiplicity of the tolerant load was significantly higher than that in the control group and remained so in the long term. The neocortex of the control group animals was characterized by the development of pathomorphological changes. After 21 days, these signs persisted. No sign of nervous tissue edema was detected in the early period after the BMA injection. A clear architectonics of the neocortex neurocyte layers were preserved.

**Conclusion:** Allogeneic biomaterial has a positive systemic effect on the organism. Also, neuroprotective and immunomodulating effects have been recorded.

**Keywords:** Allogeneic biomaterial, Cerebral cortex, Forced swimming, Neuroprotection, Rats

**Article info:**

Received: 23 Jun 2024

Accepted: 15 Sep 2024

Publish: 01 Jan 2025

**\* Corresponding Author:**

Alexey Viktorovich Prusakov, Assistant Professor.

**Address:** Federal State Budgetary Educational Institution of Higher Education, Saint Petersburg State University of Veterinary Medicine, Saint Petersburg, Russia.

**Phone:** +7 (812) 388-36-31 **E-mail:** [pseudopyos@mail.ru](mailto:pseudopyos@mail.ru)



Copyright © 2025 The Author(s).  
This is an open access article distributed under the terms of the Creative Commons Attribution License (CC-BY-NC: <https://creativecommons.org/licenses/by-nc/4.0/legalcode.en>), which permits use, distribution, and reproduction in any medium, provided the original work is properly cited and is not used for commercial purposes.

## Introduction

**A**s a rule, the highest achievements in sports competitions are associated with extreme physical and emotional stress, which imposes increased demands on health. In most cases, overwork and overtraining are superimposed on each other, giving a symptom complex of an organism's function disturbances, including the central nervous system (CNS), which can be considered a neurosis (Kholodny et al., 2021; Meftahi et al., 2023). Overfatigue disrupts the coherence of interactions between the cerebral cortex, underlying parts of the nervous system, and internal organs (Ilyin & Alvani, 2016; Jaber Al-Mamoori et al., 2022).

Allogeneic biomaterial, including skeletal muscle tissue, is known as a regeneration stimulator when applied locally (Lebedeva et al. 2019a). However, studies of systemic influence, remote action, and feedback have not previously been conducted. To identify the pharmacological effects of the allogeneic biomaterial on the central nervous system, the behavioral despair test or Porsolt forced swimming test (forced swimming to complete fatigue with a load that reflects the state of depression of the animals) was performed. This complex, severe stress test combines physical and emotional components (Khabibullin et al. 2019). This research aimed to study the experimental animals' cerebral cortex structure after forced physical activity and allogeneic biomaterial use.

## Materials and Methods

The experiment involved mature male Wistar rats weighing 200–240 g (n=20). The rats were kept in plastic cages at 22–24 °C, fed with pelleted mixed fodder. Water was supplied ad libitum. Before starting the forced swimming test, all experimental rats were allowed to swim for 3 days without a load for 10 minutes once a day.

The model of anaerobic physical activity was chosen as the method of forced swimming of rats until complete fatigue with a load—the Porsolt test, or the despair test (Zhou et al., 2021) in modification (patent for invention No. 261706 dated April 21, 2017). The swimming test was conducted daily for 30 consecutive days, from 9:00 to 11:00 AM. The weight of the animals was measured daily. The weight of the load was selected following the weighing results and was equal to 10% of the body weight.

In the main group (n=10), after all 30 training sessions, a dispersed allogeneic biomaterial (BMA) suspension was injected intramuscularly. One vial (10 mg) was diluted in 5 mL of saline for a 0.2% concentration. A total of 8 intramuscular single injections were made into the muscles of the thoracic limbs, including the shoulder biceps (m. biceps brachii), the superficial muscles of the forearm flexors, the ulnar and radial flexors of the wrist (m. flexor carpi ulnaris, m. flexor carpi radialis), and the pelvic limbs (gastrocnemius (m. triceps surae), and quadriceps femoris (m. quadriceps femoris). Then, 0.5 mL of BMA suspension was injected (4 mL). The dose of BMA was chosen arbitrarily. As BMA dispersed form, the alloplant biomaterial was used with a particle size of 50–80 µm. The alloplant biomaterial was developed at the All-Russian Center for Eye and Plastic Surgery, Ministry of Health of the Russian Federation, Ufa. The biomaterial is manufactured following the technical specifications 42-2-537-87, certified and approved for use in clinical practice by order of the Ministry of Health of the USSR No. 87 901-87 of July 22, 1987. For the present study, BMA was made from the extracellular matrix of rat tendons. In the control group (n=10), the animals were injected with physiological saline in similar zones and at the same volume.

Five and twenty-one days after the injections, a tolerance load test was performed, and swimming time (minutes) was recorded. After that, the animals were killed by insufflation of a chloroform vapor lethal dose (695 mg/kg) (Customs Documents, 2024). Next, decapitation and extraction of the brain were carried out. For histological examination, tissue pieces of the precentral gyrus were fixed in a 10% neutral formalin solution, dehydrated in increasing alcohol concentrations, and embedded in paraffin according to the generally accepted method. Histological sections were prepared on a LEICA RM 2145 microtome (Germany) and stained with hematoxylin and eosin (H&E).

Four-µm thick paraffin sections were stained using a Leica Microsystems Bond™ immunohistostainer (Germany) for immunohistochemical studies. The primary antibodies used were CD 68 diluted at 1:300 (ED1 clone), Gfap at 1:300, and bcl-2 (Santa Cruz Biotechnology, USA). The indirect streptavidin-biotin detection system Leica BOND (Novocastra™, Germany) was used for staining (Ozawa, 2019; Magaki et al., 2019; Sukswai & Khoury, 2019; Moreno et al., 2022; Prichard, 2014).

For electron microscopic examination, tissue pieces were fixed in 2.5% glutaraldehyde solution prepared in cacodylate buffer (pH 7.2–7.4) with additional fixation

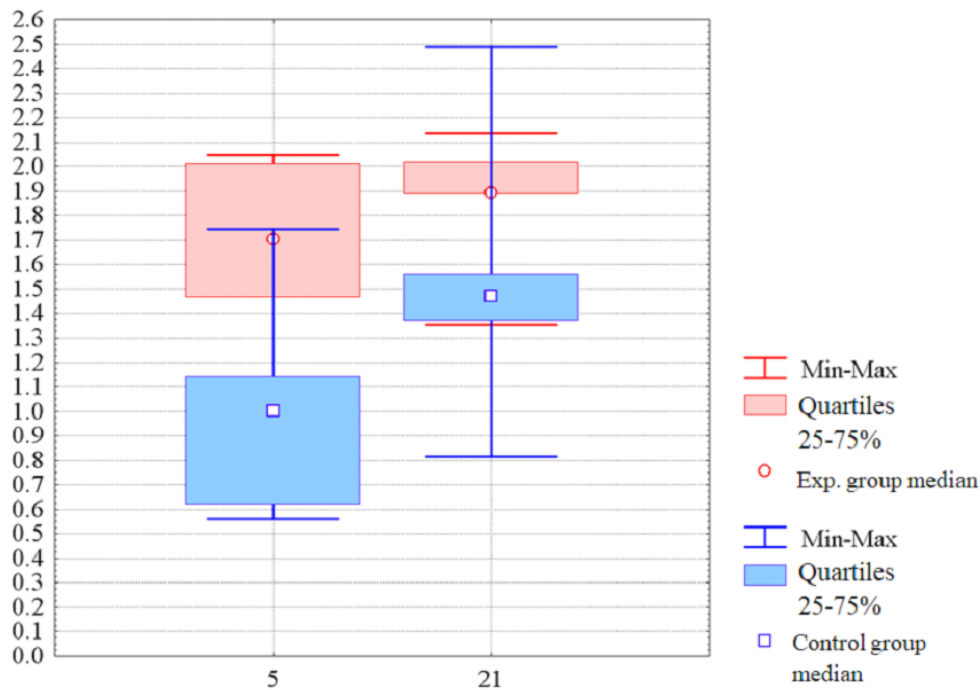


**Figure 1.** Multiplicity of swimming duration in rats after exhausting physical activity under conditions of intramuscular injection of BMA (experimental group) and saline (control group)

Notes: The x-axis shows the number of days after BMA administration. On the y-axis, the multiplicity in fractions of a unit.

in 1% OsO<sub>4</sub> solution in the same buffer. The material was dehydrated in alcohols of increasing concentration and poured into Epon-812 according to the generally accepted method. One- $\mu$ m thick semithin sections were preliminarily prepared and stained with toluidine blue in a 2.5% anhydrous soda solution. In these sections, areas for electron microscopic examination were selected. Semithin and ultrathin sections were prepared on an EM UC 7 ultramicrotome (Leica, Germany). Ultrathin sections were counterstained with a 2% aqueous solution of uranyl acetate and lead citrate, according to Reynolds, and studied under a JEM-1011 transmission microscope (Jeol, Japan) at an accelerating voltage of 80 kV (Con-dello et al., 2013; Kim et al., 2021; Klang et al., 2013).

Cells were counted in 20 fields of view for each sample. The examination and visualization of samples were carried out using a Leica DMD 108 microscope (Germany) with specialized software for controlling settings and image capture. Kruskal-Wallis rank analysis of variance was used: Median (Me) and quartiles (Q1 - 25%; Q3 - 75%), and the Mann-Whitney test to compare the results of individual observation periods within one series of experiments or between them (Schlattmann et al., 2019). Differences were considered statistically significant at  $P < 0.05$ . The SPSS software, version 10 was used for all analyses.

## Results

In the experimental group after the administration of BMA, after 5 days, the Me level of multiplicity was significantly ( $Z=2.17$ ,  $P < 0.04$ ) higher than in the control group: Me=1.70 (Q1=1.46, Q3=2.01) and Me=1 (Q1=0.62, Q3=1.14). After 21 days in the experimental and control groups, the level of multiplicity increased (Me=1.88; Q1=1.88, Q3=2.02, and Me=1.47; Q1=1.37, Q3=1.56), but it was not significant ( $Z=0.96$ ,  $P > 0.37$  and  $Z=1.85$ ,  $P > 0.07$ , respectively). At the same time, in the experimental group, the higher multiplicity level over the control group remained statistically significant ( $Z=2.13$ ,  $P < 0.04$ ; Figure 1)

Morphological analysis revealed that in the control group, after 5 days, in the cerebral cortex of the precentral gyrus, all the cell layers characteristic of the cerebral cortex were traced. However, there were many hyperchromic pyknotic nerve cells of medium and small sizes with a dense, elongated nucleus and jagged edges, containing a dense osmiophilic nucleoplasm, in which signs of chromatin disorganization and condensation were revealed. The optically dark cytoplasm contained hypertrophied Golgi complexes with dilated canals, signs of secretion stagnation, and condensation of the granular cytoplasmic reticulum. These cells were often

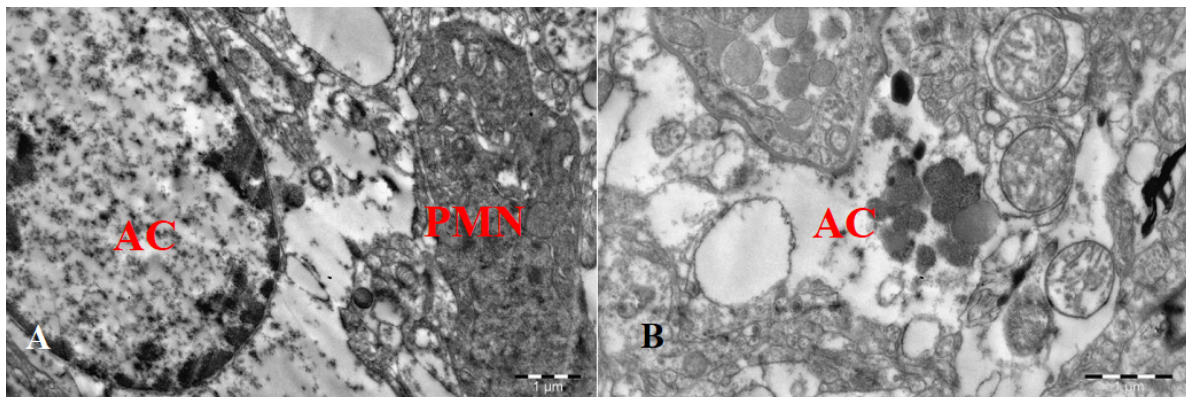


**Figure 2.** Edema of astrocytes in the cerebral cortex of the precentral gyrus of a rat after forced swimming and intramuscular injection of saline after 5 days

A) Contact of an astrocyte (AC) and pyknotic neuron (PMN), B) Swelling of the terminal pedicles of astrocytes (AC) (electronogram)

detected in direct contact with macroglial cells and astrocytes. The perinuclear cytoplasm in these cells was optically clear due to the accumulation of vacuoles and destruction, followed by the reduction of cytoplasmic organelles. In astrocytes, the body and terminal processes surrounding the capillaries were edematous and showed signs of organelle destruction. Lipofuscin inclusions (aging or “wear-and-tear” pigment) were observed in them. Also, certain sections of the basement membrane thickened many pinocytotic vesicles in the cytoplasm of endothelial cells and pericytes, microvesicular bodies, which is not typical for the norm. The capillary lumen was not free; it was filled with cell fragments and various inclusions (Figure 2). Consequently, signs of pericellular and perivascular edema were observed, evidence of a breach of the blood-brain barrier.

The neurocyte profiles were sharply expanded, the organelles were vacuolized, and the mitochondria were enlarged and rounded with partial cristae fragmentation. The synaptic apparatus was poorly developed (Figure 3).

In the inner pyramidal layer, along with a small number of hyperchromic neurocytes, light cells were observed, shadows (“melting neurons”), which arose as a result of their chromatolysis (irreversible necrobiotic changes). Microglial cells were often detected in close contact with necrobiotically altered neurocytes, such as Betz cells.

Twenty-one days after the intramuscular injection of physiological saline, signs of trophic disorders in the blood-brain barrier persisted. Destruction of lamellar structures and accumulation of aging pigment were determined in neurons. Apoptotic-altered cells and glial

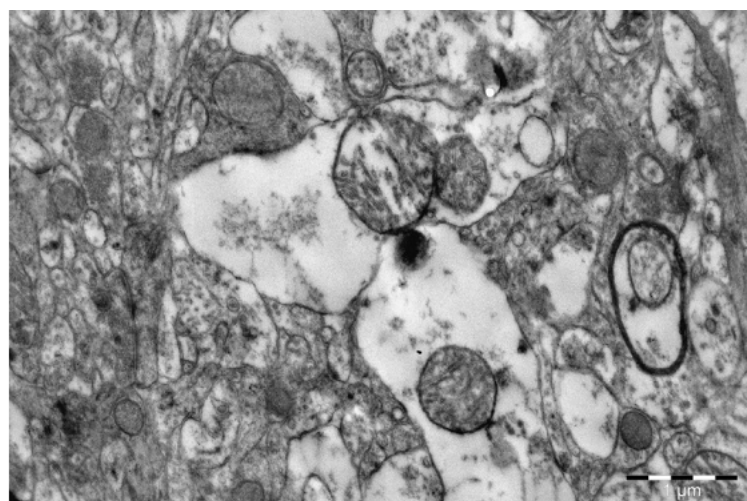


**Figure 3.** Vacuolization of the neuropile in the precentral gyrus' cerebral cortex after forced swimming and intramuscular injection of saline after 5 days (electronogram)

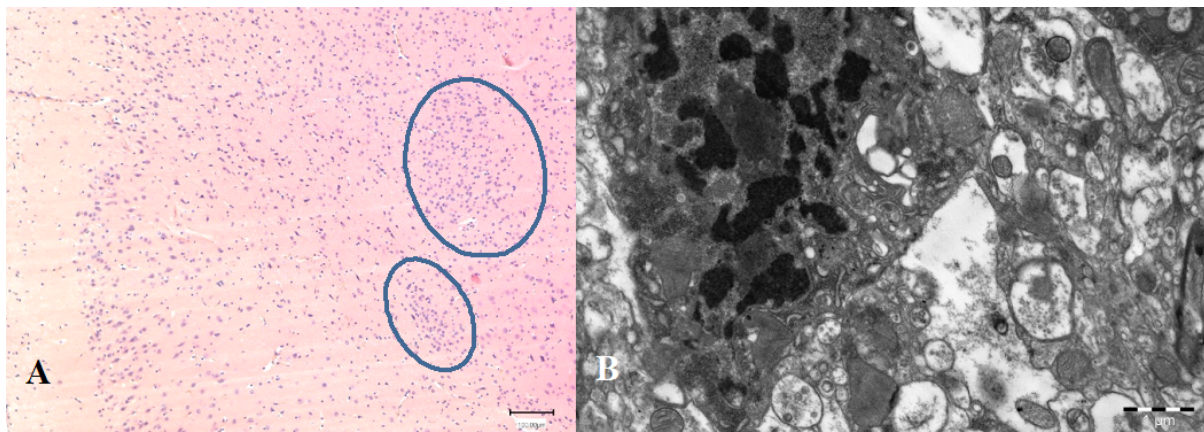


**Figure 4.** Morphological changes in the nervous tissue in the precentral gyrus after forced swimming and intramuscular injection of saline after 21 days

A) Focal proliferation of glial cells (H&E staining), B) Apoptosis of the hyperchromic neurocyte (electronogram)

proliferation were noted. All layers of neurons in the cerebral cortex were viewed. The outer granular layer was thinned and sparse—zones of local accumulation of glial cells and scars formed in the surrounding brain tissue. Neurocytes were detected in a state of programmed cell death or apoptosis. The nuclei of these cells were hyperchromic with condensed clumps, and euchromatin was absent. An increased electron density marked the cytoplasm due to ribosomal dispersion. The cisternae of the Golgi complex are vacuolated, sharply dilated, and elongated. Their hypertrophy was observed. Mitochondria are darkly destroyed, and cristae are not determined. The cytoplasm contained numerous phagosomes and residual bodies (Figure 4).

After 5 days, no pathomorphological signs in the form of cell edema and inflammatory cell infiltration were detected in the autopsy material of the cerebral cortex of rats in the experimental group. Identifying all the layers characteristic of the cerebral cortex on histological samples was possible. Pyramidal normochromic neurocytes showed mosaic structural and functional activity in this period. On the one hand, the nucleus was large, outlined by a clear double karyolemma, in which nuclear pores were revealed. Euchromatin uniformly filled the entire karyoplasm. In the cytoplasm, mitochondria of various sizes were found, from rounded to elongated. The lamellar cristae were parallel.

On the other hand, they were swollen and destroyed in places. The mitochondrial matrix is light and moderately edematous. Signs of hyperplasia were determined in the lamellar Golgi complex. Also, both ribosomal rosettes and free ribosomes were observed in the cytosol. The morphological characteristics of these cells' nuclear ele-

ments and cytoplasm are linked to their enhanced functional activity. These neurons formed contact with each other (Figure 5).

Twenty-one days after the intramuscular injection of BMA, the layers of neurocytes of the cerebral cortex were visible. There were no signs of edematous phenomena in the perivascular and pericellular spaces. The neuropil is dense, not sparse. The hemocapillaries had a dense, well-defined basement membrane that formed splits. Pericytes were located in these duplications. The perivascular space was free from pathological changes and inclusions. The end legs of astrocytes adjoined to the basement membrane, tightly covering the hemocapillaries and forming a sleeve. Numerous axon-dendritic and axon-axon synapses were noted in the perivascular field (Figure 6).

Immunohistochemical determination of some functionally significant cells revealed that on the fifth day of observation, the number of GFAP<sup>+</sup> cells in the main group was significantly lower than in the control groups ( $Z=3.7$ ;  $P<0.0001$ ). On the 21<sup>st</sup> day, in the experimental and control groups, there was a significant, sometimes double ( $Z=2.1 \div Z=4.92$ ;  $P<0.04 \div P<0.0001$ , respectively) decrease in the number of GFAP-cells. However, when using BMA, the level of GFAP cells was remarkably lower than in the control group ( $Z=3.0$ ,  $P<0.002$ ). GFAP is manifested in the cytoplasm of astrocytes, which perform a trophic, supporting role, form the glial membrane and the blood-brain barrier, and isolate the receptive surfaces of neurons from extraneous afferent influences but do not conduct nerve impulses (Flanagan et al. 2017; Aziz Anah & Aziz Anah, 2023). A reparative function consists of the proliferation and replacement of

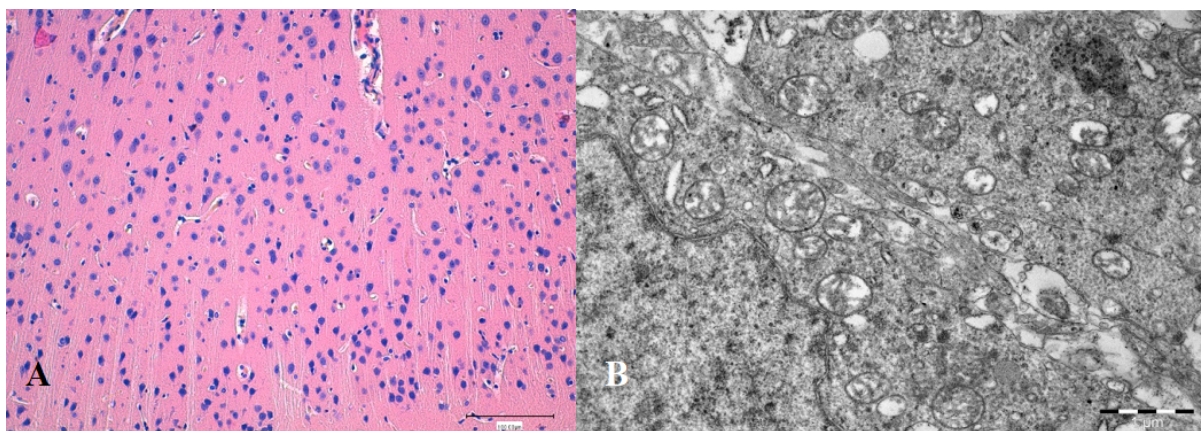


**Figure 5.** Structure of the rat precentral gyrus 5 days after forced swimming and BMA injection

A) Cerebral cortex (H&E staining), B) Interneuronal contacts (electronogram)

dead nerve cells. Therefore, it is a marker of gliosis in the cerebral cortex.

After 5 days, the levels of Bcl-2<sup>+</sup> cells in the main group were significantly ( $Z=3.5 \div Z=4.25$ ;  $P<0.0005 \div P<0.0001$ , respectively) higher than in the control groups. On the 21<sup>st</sup> day, the number of Bcl-2<sup>+</sup> cells in the main group increased ( $Z=4.0$ ,  $P<0.0001$ ). In the control group, the number of Bcl-2<sup>+</sup> cells, on the contrary, remarkably decreased ( $Z=2.18$ ,  $P<0.03$ ). Bcl-2 suppresses apoptosis in many cellular systems, including lymphohematopoietic and neuronal cells. These cells regulate cell death by controlling mitochondrial membrane permeability (Elgendy et al., 2022).

On the fifth day, the number of CD-68<sup>+</sup> cells in the main group was significantly ( $P<0.004$ ) higher than in the control group. On the 21<sup>st</sup> day in the main group, the number of CD-68<sup>+</sup> cells increased remarkably ( $Z=5$ ,  $P<0.0001$ ). In the control group, on the contrary, there were no significant changes ( $Z=1.1 \div Z=0.1$ ,  $P>0.24 \div 0.93$ ) and, as a result, remarkable excess ( $Z=5.49 \div Z=5.83$ ,  $P<0.0001$ ) of the main group data over the control group became even more contrasting. CD-68 is a phagocytic macrophage marker. They are microsialin, an enzyme of secondary lysosomes. CD-68 in the cerebral cortex was found in microglial cells (Stankov et al., 2015).

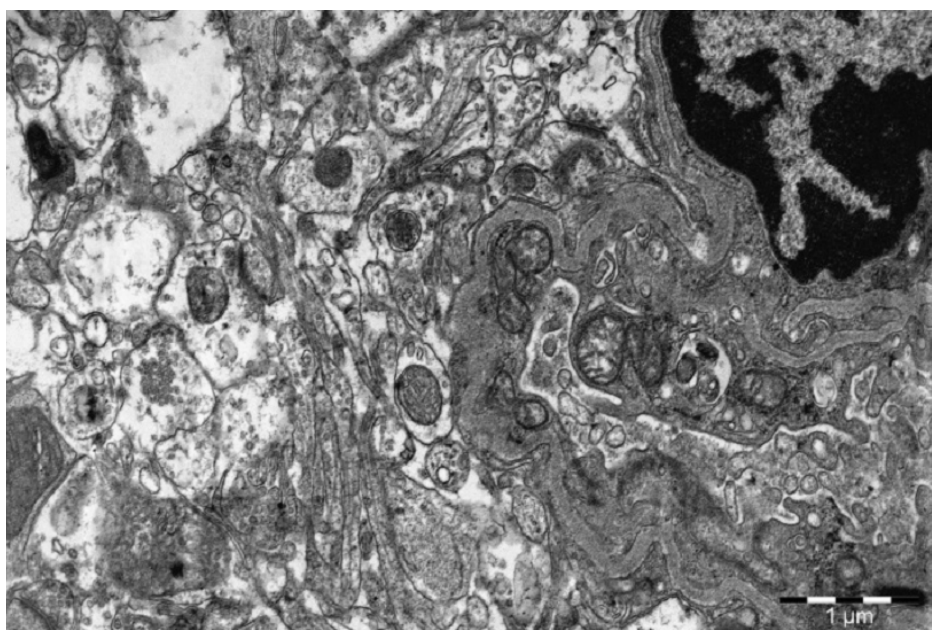


**Figure 6.** Neuropile and hemocapillaries 21 days after forced swimming and intramuscular injection of BMA (electronogram)

**Table 1.** The number of GFAP<sup>+</sup>, Bcl-2<sup>+</sup>, CD-68<sup>+</sup> Cells, and shadow cells on the fifth and twenty-first days of observation

Group	Median			
	Cell Type			
	GFAP <sup>+</sup>	Bcl-2 <sup>+</sup>	CD-68 <sup>+</sup>	Shadow Cells
Experimental group (5 <sup>th</sup> day)	15 (13, 18)	22.5 (20, 25)	1 (0, 2)	14 (12, 18)
Experimental group (21 <sup>st</sup> day)	9 (7, 11)	31 (27, 34)	3 (2, 3)	3 (3, 5)
Control group (5 <sup>th</sup> day)	26 (21, 28)	8.5 (6, 12)	0.5 (0, 1)	21 (10, 36)
Control group (21 <sup>st</sup> day)	13 (11, 15)	6 (5, 7)	1 (0, 2)	18 (9, 23)

The number of shadow cells in the main group decreased significantly with time ( $Z=3.1$ ,  $P<0.002$ ). It turned out to be a multiple and significantly lower than in the control group at all times of observation ( $Z=5.56 \div Z=5.68$ ,  $P<0.0001$ ) (Table 1).

## Discussion

BMA is a cell-free extracellular matrix of allogeneic origin and contains collagen, glycosaminoglycans, and proteoglycans (Lebedeva et al., 2019). Its pharmacological action stimulates tissue regeneration when applied locally, which activates angiogenesis, causes chemoattraction of mesenchymal stem cells, and stimulates their differentiation, followed by induction into tissue-specific tissues. Also, it is an inhibitor of fibrosis during the healing of various tissues (Lebedeva et al., 2021; Lebedeva et al., 2018). BMA exerts its range of influences through the system of mononuclear phagocytes, M1 macrophages, which migrate in response to biomaterial implantation and phagocytize it, acquiring a special phenotype. BMA is an immunostimulator of the cellular link of immunity (Lebedeva et al., 2019b). The remote effect of BMA biodegradation products has not been studied to date. It can be assumed that in response to the introduction of BMA into the muscle tissue of the upper and lower extremities, which were subjected to intense physical activity, they showed an actoprotective effect, which is confirmed by an increase in the level of the tolerant load multiplicity compared to the control group (Baryshev et al., 2022; Kuznetsov et al., 2022; Pomamarev et al., 2022). Normoxic muscle tissues can also contribute to the immune-adaptive defense of various tissues, including the nervous. CD-68 macrophages in nervous tissue have a similar effect by suppressing tissue gliosis. Recovery, stabilization, or stimulation of angiogenesis takes place, and this is observed in the main group. Due to this effect, neurohumoral homeostasis is maintained; it has a neuroprotective effect and leads to a decrease in

chromatolysis in neurocytes, which is confirmed by an increase in the number of Bcl-2<sup>+</sup> cells in the main group and, consequently, a decrease in the number of GFAP<sup>+</sup> and shadow cells.

## Conclusion

Forced anaerobic physical activity contributed to the development of pathomorphological changes in the nervous tissue of the cerebral cortex in the precentral gyrus. Signs of cell edema, neuropil, perivascular pool, and synaptic apparatus inactivation in the control group were determined. Pyknosis and chromatolysis of neurocytes ended with focal gliosis. Moreover, these signs persisted for 21 days. The number of GFAP<sup>+</sup> cells and shadow cells increased. Also, the number of Bcl-2<sup>+</sup> cells was reduced compared to the main group.

Five days after the injection of BMA under prolonged forced swimming with a load, no signs of edema of the nervous tissue were detected. The layers of neurocytes of the cerebral cortex retained a distinct architectonics. Synaptic activity was noted. Structural features of neurocytes also indicated their functional viability: restoration of energy balance, activation of biosynthetic processes and secretory activity, as well as their cooperation. The content of CD68<sup>+</sup> macrophages increased.

Therefore, based on the results, the allogeneic biomaterial has a systemic effect on the animal organism. It has actoprotective, neuroprotective, and immunomodulatory effects when locally injected into muscles.

## Ethical Considerations

### Compliance with ethical guidelines

This work was approved by Bashkir State Medical University Ufa, Russia (No.: 056-00124-21-00; Dated: 12/23/2020).

## Funding

This study was funded by the Strategic Academic Leadership Program of the [Bashkir State Medical University](#), Ufa, Russia (Code: PRIORITET-2030).

## Authors' contributions

All authors contributed equally to the conception and design of the study, data collection and analysis, interpretation of the results and drafting of the manuscript. Each author approved the final version of the manuscript for submission.

## Conflict of interest

The authors declared no conflict of interest.

## References

- Aziz Anah, S., & Aziz Anah, S. (2023). New Recording of *Toxoplasma gondii* in Wild *Tortoise Testudo graeca* using Nested PCR Method. *Archives of Razi Institute*, 78(3), 1029-1034. [PMID]
- Baryshev, V. A., Popova, O. S., & Ponamarev, V. S. (2022). New methods for detoxification of heavy metals and mycotoxins in dairy cows. *Online Journal of Animal and Feed Research*, 12(2), 81-88. [DOI:10.51227/ojaf.2022.11]
- Condello, M., Caraglia, M., Castellano, M., Arancia, G., & Meschini, S. (2013). Structural and functional alterations of cellular components as revealed by electron microscopy. *Microscopy Research and Technique*, 76(10), 1057-1069. [DOI:10.1002/jemt.22266] [PMID]
- Elgendy, W., Swelem, R., Aboudiba, N., & Elwafa, R. A. (2022). Role of MicroRNA-326 and its target genes Bcl-xL and bak as potential markers in platelet storage lesion in blood banks. *Indian Journal of Hematology and Blood Transfusion*, 38(4), 731-738. [DOI:10.1007/s12288-022-01542-0] [PMID]
- Flanagan, E. P., Hinson, S. R., Lennon, V. A., Fang, B., Aksamit, A. J., & Morris, P. P., et al. (2017). 'Glial fibrillary acidic protein immunoglobulin G as a biomarker of autoimmune astrocytopathy: Analysis of 102 patients. *Annals of Neurology*, 81(2), 298-309. [DOI:10.1002/ana.24881] [PMID]
- Ilyin, V. N., & Alvani, A. R. (2016). 'Ubiquity and formation of chronic fatigue in qualified sportsmen. *Pedagogics, Psychology, Medical-Biological Problems of Physical Training and Sports*, 20(3), 11-17. [DOI:10.15561/18189172.2016.0302]
- Jaber Al-Mamoori, A., Abdulameer Almस्ताفا, H. M. S., & Alsaffar, Y. (2022). Overexpressed toll-like receptor 2 and the influence on the severity of acute ischemic stroke. *Archives of Razi Institute*, 77(6), 2379-2384. [DOI:10.22092/ARI.2022.358615.2265]
- Khabibullin, R., Khabibullin, I., Yagafarov, R., Bakirova, A., Faizlaev, R., & Karimov, F., et al. (2019). The influence of dietary supplements on the adaptive processes in animals after physical stress. *Bulgarian Journal of Agricultural Science*, 25 (Suppl. 2), 105-118. [Link]
- Kholodny Yu, I., Malakhov, D. G., Orlov, V. A., Kartashov, S. I., Aleksandrov Yu, I., & Kovalchuk, M. V. (2021). Study of neurocognitive processes in the paradigm of information concealment. *Experimental Psychology*, 14(3), 17-39. [DOI:10.17759/exppsy.2021140302]
- Kim, H., Murata, M. M., Chang, H., Lee, S. H., Kim, J., & Lee, J. H., et al. (2021). Optical and electron microscopy for analysis of nanomaterials. *Advances in Experimental Medicine and Biology*, 1309, 277-287. [DOI:10.1007/978-981-33-6158-4\_12] [PMID]
- Klang, V., Valenta, C., & Matsko, N. B. (2013). Electron microscopy of pharmaceutical systems. *Micron (Oxford, England: 1993)*, 44, 45-74. [DOI:10.1016/j.micron.2012.07.008] [PMID]
- Kuznetsov Yu, E., Lunegov, A. M., Ponamarev, V. S., & Romashova, E. B. (2022). Correlation relationships between the content of total bile acids and the main biochemical parameters of blood in minks (*Mustela vison Schreber, 1777*). *Agricultural Biology*, 57(6), 1217-1224. [DOI:10.15389/agrobiol.2022.6.1217eng]
- Lebedeva, A. I., Muslimov, S. A., Afanasiev, S. A., & Kondratieva, D. S. (2019). The role of macrophages in the regeneration of muscle tissue induced by allogeneic biomaterial. *Russian Journal of Immunology*, 22(2-2), 849-851. [DOI:10.31857/S102872210006676-8]
- Lebedeva, A. I., Muslimov, S. A., Gareev, E. M., Popov, S. V., & Afanasiev, S. A. (2018). 'Stimulation of autologous progenitor and committed cells in ischemic damaged myocardium. *Russian Journal of Cardiology*, 23(11), 123-129. [DOI:10.15829/1560-4071-2018-11-123-129]
- Lebedeva, A. I., Muslimov, S. A., Gareev, E. M., Popov, S. V., Afanasiev, S. A., & Kondratieva, D. S. (2021). 'Allogeneic biomaterial as an inductor of regeneration in the myocardium injured by experimental ischemia. *Pathological Physiology and Experimental Therapy*, 65(1), 60-69. [DOI:10.25557/0031-2991.2021.01.60-69]
- Lebedeva, A. I., Muslimov, S. A., Vagapova, V. Sh., & Shcherbakov D. A. (2019). 'Morphological aspects of regeneration of skeletal muscle tissue induced by allogeneic biomaterial. *Practical Medicine*, 17(1), 98-102. [DOI:10.32000/2072-1757-2019-1-98-102]
- Magaki, S., Hojat, S. A., Wei, B., So, A., & Yong, W. H. (2019). An introduction to the performance of immunohistochemistry. *Methods in Molecular Biology (Clifton, N.J.)*, 1897, 289-298. [DOI:10.1007/978-1-4939-8935-5\_25] [PMID]
- Material Safety Data Sheet Chloroform MSDS (2024). ScienceLab.com Chemicals and Laboratory Equipment. Retrieved from: [Link]
- Meftahi, G. H., Hatf, B., & Pirzad Jahromi, G. (2023). Creatine activity as a neuromodulator in the central nervous system. *Archives of Razi Institute*; 78(4), 1169-1175. [DOI:10.32592/ARI.2023.78.4.1169] [PMID]



- Moreno, V., Smith, E. A., & Piña-Oviedo, S. (2022). Fluorescent Immunohistochemistry. *Methods in Molecular Biology (Clifton, N.J.)*, 2422, 131-146. [DOI:10.1007/978-1-0716-1948-3\_9] [PMID]
- Ozawa, H. (2019). [Principles and basics of immunohistochemistry (Japanese)]. *Nihon Yakurigaku Zasshi*, 154(4), 156-164. [DOI:10.1254/fpj.154.156] [PMID]
- Ponamarev, V., Yashin, A., Prusakov, A., & Popova, O. (2022). Influence of modern probiotics on morphological indicators of pigs' blood in toxic dyspepsia. In A. Ronzhin, & A. Kostyaev (Eds), *Agriculture digitalization and organic production. Smart Innovation, Systems and Technologies*. Singapore: Springer. [DOI:10.1007/978-981-19-7780-0\_12]
- Prichard, J. W. (2014). Overview of automated immunohistochemistry. *Archives of Pathology & Laboratory Medicine*, 138(12), 1578-1582. [DOI:10.5858/arpa.2014-0083-RA] [PMID]
- Customs Documents. (2024). Recommendation of the EEC dated November 14, 2023 No. 33 "On the Guidelines for working with laboratory (experimental) animals when conducting preclinical (non-clinical) studies. Retrieved from: [Link]
- Schlattmann, P., Scherag, A., Rauch, G., & Mansmann, U. (2019). [The role of biostatistics in institutional review boards (German)]. *Bundesgesundheitsblatt, Gesundheitsforschung, Gesundheitsschutz*, 62(6), 751-757. [DOI:10.1007/s00103-019-02951-9] [PMID]
- Stankov, A., Belakaposka-Srpanova, V., Bitoljanu, N., Cakar, L., Cakar, Z., & Rosoklija, G. (2015). Visualization of microglia with the use of immunohistochemical double staining method for CD-68 and Iba-1 of cerebral tissue samples in cases of brain contusions. *Prilozi (Makedonska akademija na naukite i umetnostite. Oddelenie za medicinski nauki)*, 36(2), 141-145. [DOI:141-145. 10.1515/prilozi-2015-0062] [PMID]
- Sukswai, N., & Khoury, J. D. (2019). Immunohistochemistry innovations for diagnosis and tissue-based biomarker detection. *Current Hematologic Malignancy Reports*, 14(5), 368-375. [DOI:10.1007/s11899-019-00533-9] [PMID]
- Zhou, Y., Yan, M., Pan, R., Wang, Z., Tao, X., & Li, C., et al. (2021). Radix Polygalae extract exerts antidepressant effects in behavioral despair mice and chronic restraint stress-induced rats probably by promoting autophagy and inhibiting neuroinflammation. *Journal of Ethnopharmacology*, 265, 113317. [DOI:10.1016/j.jep.2020.113317] [PMID]

This Page Intentionally Left Blank